Supporting Information

Robust Bioinspired Graphene-based Nanocomposites via Synergistic Toughening of Zinc Ions and Covalent Bonding

Shanshan Gong, Lei Jiang and Qunfeng Cheng*

Key Laboratory of Bio-inspired Smart Interfacial Science and Technology of Ministry of Education, School of Chemistry and Environment,

Beihang University Beijing 100191, P. R. China

*Correspondence should be addressed to Qunfeng Cheng, E-mail: cheng@buaa.edu.cn

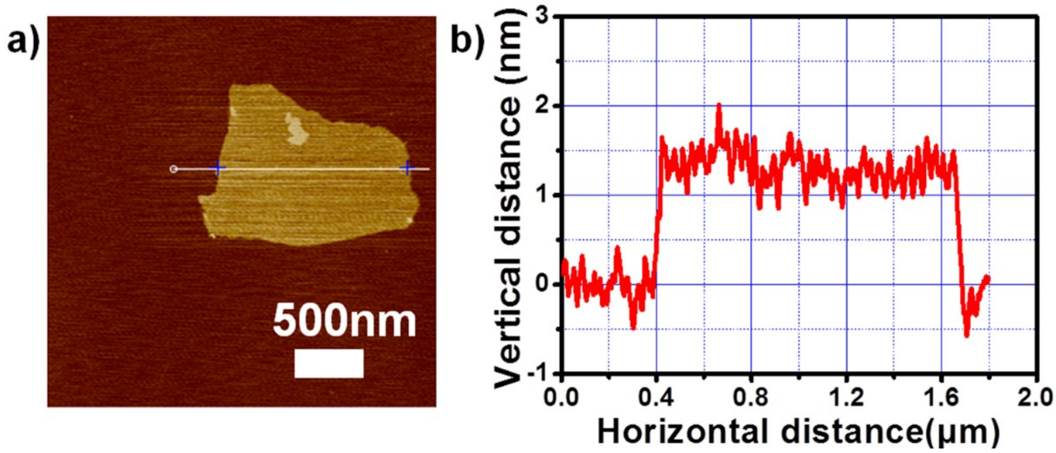

Figure S1. a) AFM image of the as-prepared GO nanosheets on the mica substrate and b) the thickness of GO nanosheet is about 1.0 nm.

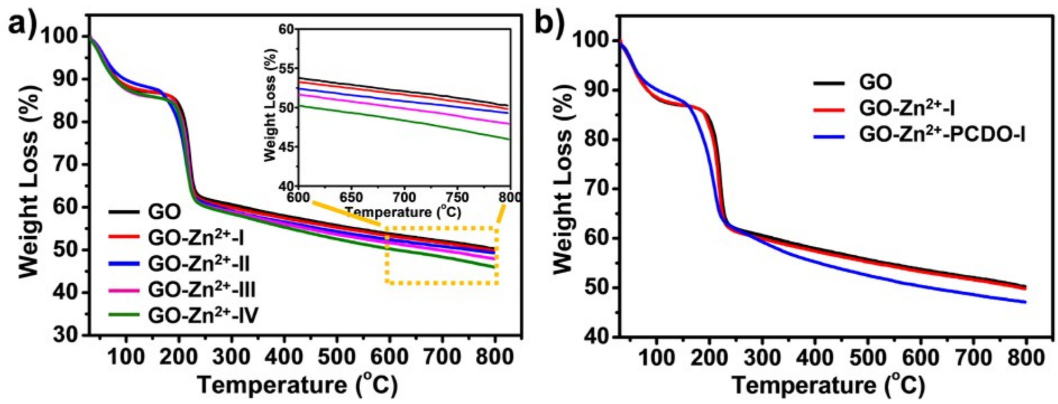

Figure S2. a) and b) TGA curves of pure GO film, GO-Zn^{2+} hybrid layered materials and GO-Zn^{2+}-PCDO-I nanocomposites. The curves were obtained under the atmosphere of nitrogen with a temperature rising rate of 10 $K \cdot min^{-1}$.

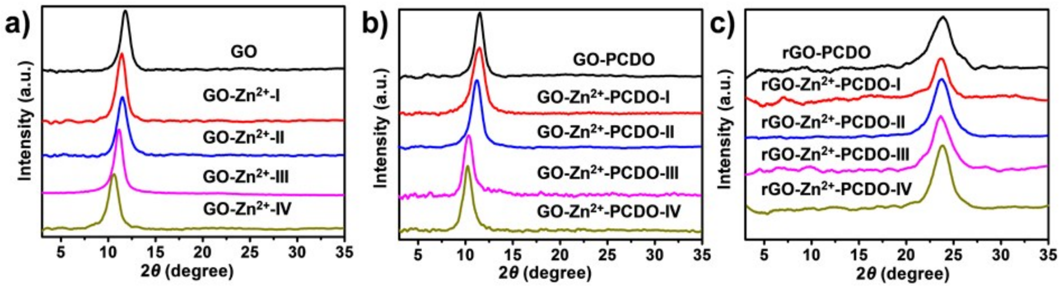

Figure S3. XRD spectra of GO-Zn^{2+} (a), GO-Zn^{2+}-PCDO (b), and rGO-Zn^{2+}-PCDO (c) nanocomposites with different Zn^{2+} contents. The *d*-spacing of the nanocomposites rises with the increasing of Zn^{2+} content.

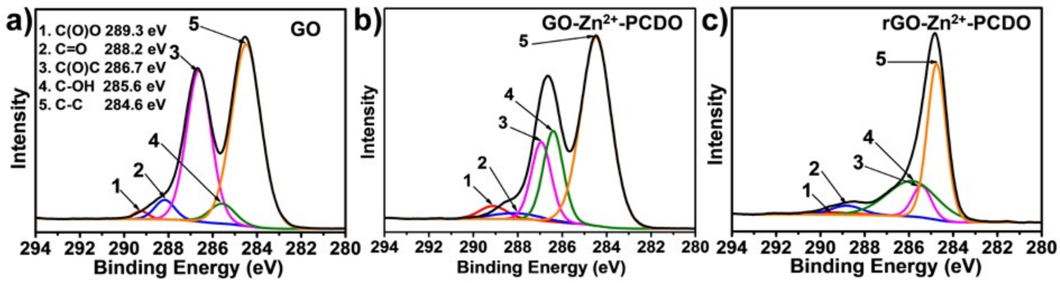

Figure S4. XPS spectra of pure GO film (a), GO-Zn^{2+}-PCDO nanocomposites (b) and rGO-Zn^{2+}-PCDO nanocomposites (c), respectively. The decreasing of the peak intensity of C=O and C-O after HI reduction shows the removal of the unreacted functional groups.

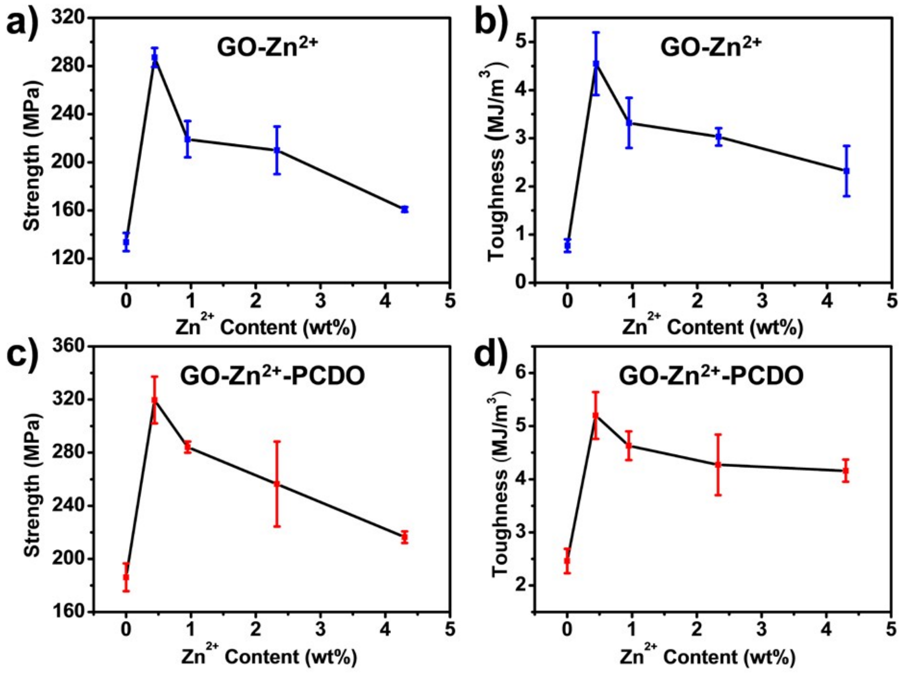

Figure S5. The tensile strength and toughness of GO-Zn^{2+} nanocomposites (a) and (b), GO-Zn^{2+}-PCDO nanocomposites (c) and (d) with different contents of Zn^{2+}.

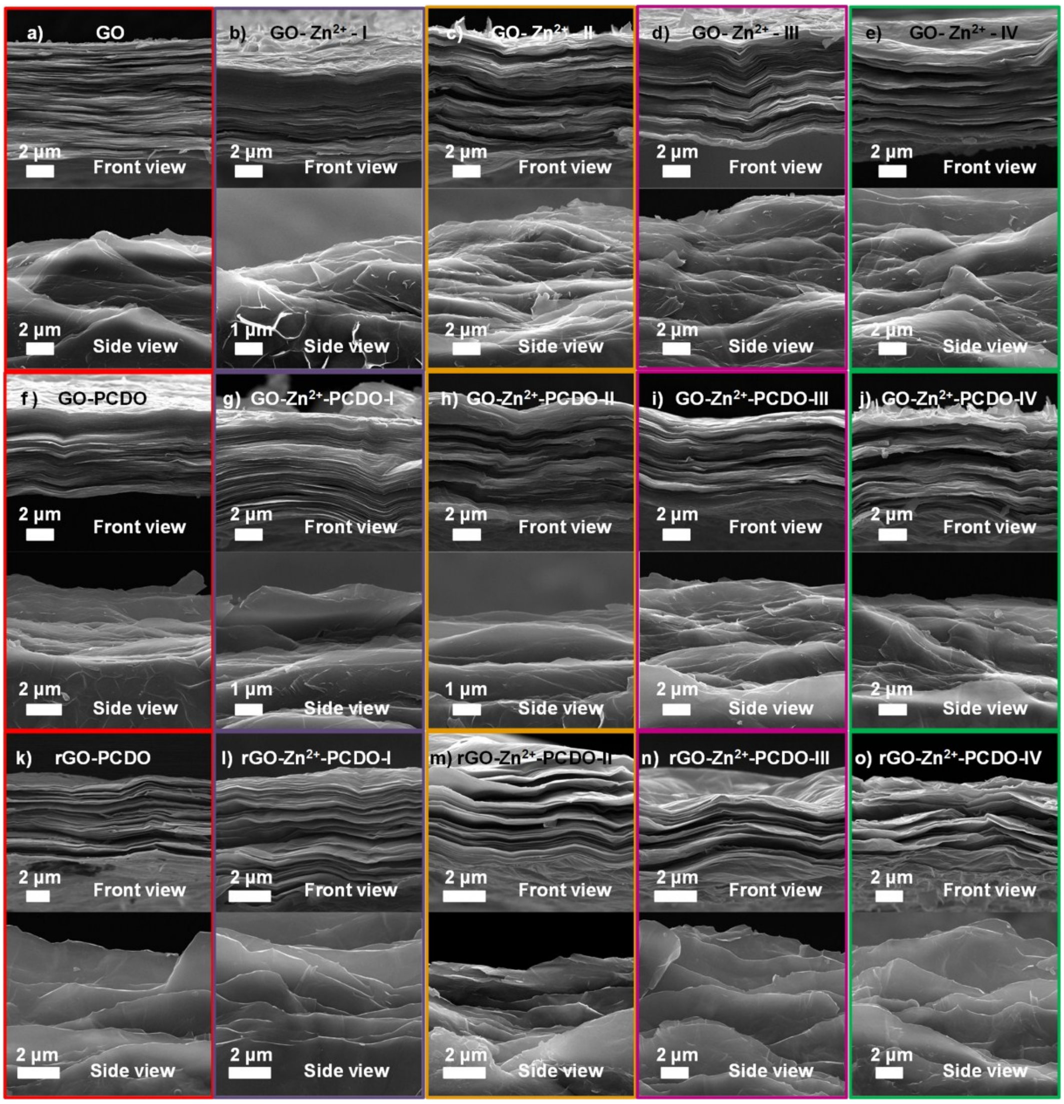

Figure S6. The front and side view fracture morphologies of pure GO film, GO-Zn^{2+}, GO-PCDO, GO-Zn^{2+}-PCDO, rGO-PCDO and rGO-Zn^{2+}-PCDO nanocomposites, respectively. a) GO film, b) GO-Zn^{2+}-I, c) GO-Zn^{2+}-II, d) GO-Zn^{2+}-III, e) GO-Zn^{2+}-IV, f) GO-PCDO, g) GO-Zn^{2+}-PCDO-I, h) GO-Zn^{2+}-PCDO-II, i) GO-Zn^{2+}-PCDO-III, j) GO-Zn^{2+}-PCDO-IV, k) rGO-PCDO, l) rGO-Zn^{2+}-PCDO-I, m) rGO-Zn^{2+}-PCDO-II, n) rGO-Zn^{2+}-PCDO-III, o) rGO-Zn^{2+}-PCDO-IV nanocomposites.

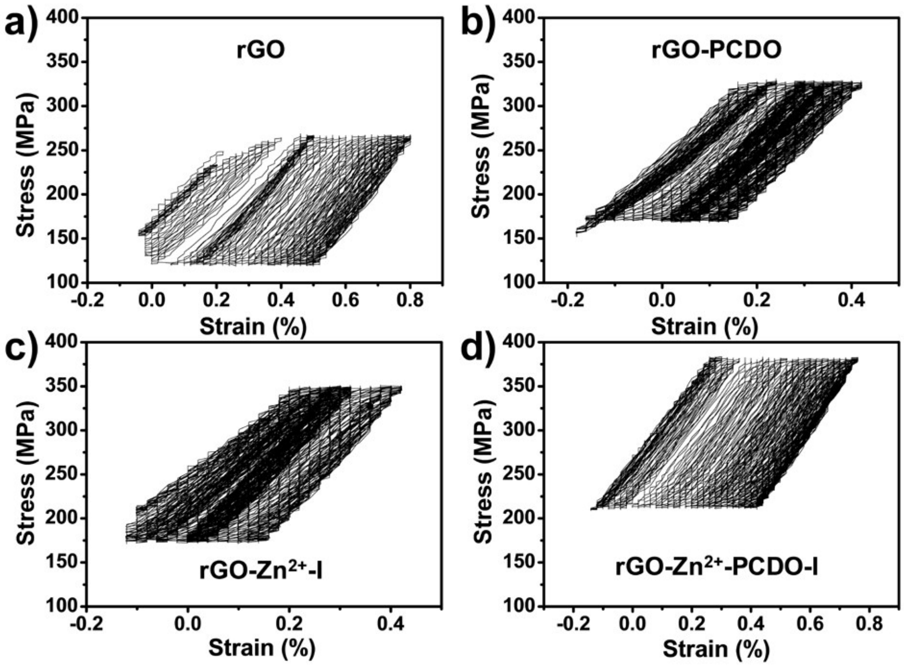

Figure S7. The stress-strain fatigue curves of rGO film (a), rGO-PCDO nanocomposites (b), rGO-Zn^{2+}-I nanocomposites (c) and rGO-Zn^{2+}-PCDO-I nanocomposites (d), demonstrating the resultant rGO-Zn^{2+}-PCDO-I nanocomposites have excellent fatigue resistance property, superior to rGO film, rGO-PCDO and rGO-Zn^{2+}-I nanocomposites.

Table S1. Zn^{2+} contents in the GO-Zn^{2+} nanocomposites were conducted by TGA, as well as PCDO content in the GO-Zn^{2+}-PCDO-I nanocomposites.

Sample	Input Zn^{2+} contents (wt%)	Zn^{2+} contents by TGA (wt%)	PCDO content by TGA (wt%)
GO	0.00	0.00	--
GO-Zn^{2+}-I	0.50	0.44	--
GO-Zn^{2+}-II	1.00	0.95	--
GO-Zn^{2+}-III	3.00	2.33	--
GO-Zn^{2+}-IV	5.00	4.30	--
GO-Zn^{2+}-PCDO-	0.50	0.44	2.68

Table S2. The *d*-spacing of the pure GO film, GO-Zn^{2+} nanocomposites, GO-Zn^{2+}-PCDO nanocomposites and rGO-Zn^{2+}-PCDO nanocomposites with different contents of Zn^{2+}.

Sample	**2θ (º)**	***d*-spacing (Å)**
GO	11.76	7.52
GO-Zn^{2+}-I	11.52	7.68
GO-Zn^{2+}-II	11.44	7.73
GO-Zn^{2+}-III	11.18	7.92
GO-Zn^{2+}-IV	10.62	8.32
GO-PCDO	11.50	7.69
GO-Zn^{2+}- PCDO-I	11.44	7.73
GO-Zn^{2+}-PCDO-II	11.36	7.78
GO-Zn^{2+}-PCDO-III	10.40	8.50
GO-Zn^{2+}-PCDO-IV	10.26	8.61
rGO-PCDO	23.88	3.72
rGO-Zn^{2+}-PCDO-I	23.80	3.73
rGO-Zn^{2+}-PCDO-II	23.74	3.74
rGO-Zn^{2+}-PCDO-III	23.68	3.75
rGO-Zn^{2+}-PCDO-IV	23.66	3.76

Table S3. Mechanical properties of pure GO film, GO-PCDO, rGO-PCDO, GO-Zn^{2+} hybrid layered materials, the GO-Zn^{2+}-PCDO and rGO-Zn^{2+}-PCDO nanocomposites.

Sample	**Tensile strength (MPa)**	**Modulus (GPa)**	**Strain (%)**	**Toughness (MJ/m^3)**
GO	133.8 ± 7.6	12.4 ± 0.2	1.1 ± 0.02	0.8 ± 0.1
rGO	213.1 ± 9.8	7.2 ± 0.2	2.7 ± 0.3	2.2 ± 0.07
GO-PCDO	186.2 ± 10.4	9.5 ± 0.5	2.8 ± 0.3	2.5 ± 0.2
rGO-PCDO	369.9 ± 10.3	8.0 ± 0.8	3.6 ± 0.3	4.3 ± 0.5
GO-Zn^{2+}-I	287.1 ± 7.9	9.4 ± 0.7	3.7 ± 0.2	4.6 ± 0.6
rGO-Zn^{2+}-I	355.6 ± 20.9	7.2 ± 0.2	4.1 ± 0.4	4.2 ± 0.9
GO-Zn^{2+}-PCDO-I	319.7 ± 17.6	11.8 ± 1.4	3.8 ± 0.4	5.2 ± 0.4
rGO-Zn^{2+}-PCDO-I	439.1 ± 15.9	11.2 ± 1.1	5.3 ± 0.2	7.5 ± 0.5
GO-Zn^{2+}-II	216.3 ± 15.2	9.5 ± 1.6	3.6 ± 0.5	3.3 ± 0.5
GO-Zn^{2+}-PCDO-II	284.1 ± 4.2	9.3 ± 0.3	3.9 ± 0.2	4.6 ± 0.3
rGO-Zn^{2+}-PCDO-II	406.8 ± 10.4	9.8 ± 0.8	5.1 ± 0.2	6.8 ± 0.2
GO-Zn^{2+}-III	210.0 ± 19.8	12.3 ± 1.0	2.7 ± 0.2	2.9 ± 0.3
GO-Zn^{2+}-PCDO-III	256.4 ± 32.0	8.4 ± 1.0	3.8 ± 0.3	4.3 ± 0.6
rGO-Zn^{2+}-PCDO-III	398.0 ± 12.1	7.5 ± 1.0	5.3 ± 0.1	6.7 ± 0.3
GO-Zn^{2+}-IV	160. 9 ± 2.0	11.2 ± 0.9	2.9 ± 0.2	2.3 ± 0.5
GO-Zn^{2+}-PCDO-IV	216.4 ± 4.4	7.3 ± 1.5	4.1 ± 0.2	4.2 ± 0.2
rGO-Zn^{2+}-PCDO-IV	363.8 ± 11.3	7.4 ± 0.2	5.1 ± 0.1	6.6 ± 0.05

Table S4. The mechanical properties of natural nacre, other graphene-based nanocomposites and the rGO-Zn^{2+}-PCDO-I nanocomposites.

Layered Materials	Stress (MPa)	Toughness (MJ/m^3)	Reference
Nacre	200	2.6	[3]
GO-PMMA	148.3	2.35	[14]
rGO-PVA	188.9	2.52	[13]
rGO-SF	300	2.8	[43]
GO-Ca^{2+}	125.8	0.31	[15]
GO-SF	292.4	3.42	[44]
GO-Mg^{2+}	80.6	0.13	[15]
GO-GA	101	0.3	[45]
GO-PAA	91.9	0.15	[47]
GO-Borate	185	0.14	[48]
GO-PEI	209.9	0.23	[46]
rGO-PCDO	129.6	3.91	[26]
rGO-PDA	204.9	4.0	[49]
rGO-MoS_2-TPU	235.3	6.9	[38]
Borate-GO-PVA	360.7	1.4	[50]
rGO-PAPB	382.0	7.50	[40]
rGO-Cu^{2+}	335	0.5	[17]
rGO-MMT-PVA	356.0	7.5	[39]
rGO-DWNTs-PCDO	374.1	9.2	[37]
GO-Fe^{3+}-TA	169.27	0.42	[42]
GO-PI-Mg^{2+}	90.6	5.04	[41]
rGO-CS	526.7	17.7	[21]
rGO-Zn^{2+}-PCDO-I	439.1	7.5	Our work

Table S5. The electrical properties of rGO film, rGO-PCDO, rGO-Zn^{2+} and rGO-Zn^{2+}-PCDO nanocomposites.

Sample	Electrical conductivity (S/cm)
rGO	153.2 ± 13.1
rGO-PCDO	168.7 ± 6.5
rGO-Zn^{2+}-I	119.6 ± 4.6
rGO-Zn^{2+}-PCDO-I	131.8 ± 4.2
rGO-Zn^{2+}-PCDO-II	126.4 ± 10.7
rGO-Zn^{2+}-PCDO-III	120.8 ± 15.1
rGO-Zn^{2+}-PCDO-IV	100.8 ± 10.5